Research in Astron. Astrophys. Vol.0 (200x) No.0, 000–000
http://www.raa-journal.org *http://www.iop.org/journals/raa*

***R**esearch in*
***A**stronomy and*
***A**strophysics*

Dependence of large SEP events with different energies on the associated flares and CMEs

Gui-Ming Le[1,2] and Xue-Feng Zhang[2]

[1] Key Laboratory of Space Weather, National Center for Space Weather, China Meteorological Administration, Beijing, 100081, China; *legm@cma.gov.cn*
[2] School of Computer Science, Anhui University of Technology, Maanshan 243032, China

Received 2017 July 10; accepted 2017 August 24

Abstract To investigate the dependence of large gradual solar energetic particle (SEP) events on the associated flares and coronal mass ejections (CMEs), the correlation coefficients (CC) between the peak intensities of E>10 MeV (I_{10}), E>30 MeV (I_{30}) and E>50 MeV (I_{50}) protons and soft X-ray (SXR) emission of associated flares and the speeds of associated CMEs in the three longitudinal areas W0-W39, W40-W70 (hereafter well connected region) and W71-W90 have been calculated respectively. The classical correlation analysis shows thst CCs between SXR emission and the peak intensities of SEP events always reach their largest value in the well connected region and then decline dramatically in the longitudinal area outside the well connected region, suggesting that may contribute to the production of SEPs in large SEP events. Both classical and partial correlation analysis show that SXR fluence is a better parameter describing the relationship between flares and SEP events. For SEP events with source location in the well connected region, the CCs between SXR fluence and I_{10}, I_{30} and I_{50} are 0.58±0.12, 0.80±0.06 and 0.83±0.06 respectively, while the CCs between CME speed and I_{10}, I_{30} and I_{50} are 0.56±0.12, 0.52±0.13 and 0.48±0.13 respectively. The partial correlation analyses show that in the well connected region, both CME shock and SXR fluence can significantly affect I_{10}, while SXR peak flux makes no additional contribution. For E>30 MeV protons with source location in the well connected region, only SXR fluence can significantly affect I_{30}, CME shock make small contribution to I_{30}, while SXR peak flux makes no additional contribution. For E>50 MeV protons with source location in the well connected region, only SXR fluence can significantly affect I_{50}, while both CME shock and SXR peak flux make no additional contribution. We conclude that these findings bring statistical evidence that for SEP events with source location in the well connected region, CME shock is only an effective accelerator for E<30 MeV protons, while flares not only are effective accelerators for E<30 MeV protons, but also for E>30 MeV protons, and E>30 MeV protons may be mainly accelerated by concurrent flares.

Key words: Sun:coronal mass ejections (CMEs)-Sun:flares-(Sun:)particle emission

1 INTRODUCTION

There are two kinds of solar energetic particle (SEP) events, named as impulsive and gradual SEP events respectively. The former is accompanied by an impulsive flare, while the latter is accompanied with both a gradual flare and a fast coronal mass ejection (CME), and the intensity-time profile of solar

proton events (SPEs) can be used to predict the geoeffectiveness of the CMEs associated with SPEs (Le et al. 2016). Nobody doubts that the solar source of an impulsive SEP event is associated impulsive flare. However, when a gradual SEP event happened, whether the concurrent flare contributed to the SEP event is still an open question. There were two kinds of point of views on the solar source of gradual SEP events. The first one is that only CME-driven shocks contributes to gradual SEP events (e.g. Reames 1999, Tylka et al. 2005). The second one is that the solar source of a gradual SEP event may be both the concurrent flare and the shock driven by the associated CME (e.g., Kallenrode 2004, Trottet et al. 2015). Cane et al. (2007) suggested that solar flares and CMEs are likely to coexist and the evolution of any event depends on relative importance of the processes. This is also consistent with the statement (Firoz, K. A., et al. 2012) that the type III and type II bursts are successive evolutions and it is difficult to separate them. Andriopoulou et al. (2011) suggested that it difficult to determine which the dominant acceleration mechanism in each GLE case is. The investigation of the properties of SEPs inferred from their associated radio emission suggests that a clear-cut distinction between flare-related and CME-related SEP events is difficult to establish (Kouloumvakos et al. 2015). Some cases and statistical studies (e.g. Miroshnichenko et al., 2005, Aurass et al., 2006, Le et al. 2006, Simnett 2006, Li et al. 2007a, 2007b, 2009, Bazilevskaya 2009, Masson et al. 2009, Grechnev et al. 2008, Perez-Peraza et al. 2009, Aschwanden 2012, Le et al. 2013, Klein et al. 2014) have shown that relativistic solar protons (RSPs) may be accelerated by the concurrent flares. Some statistical investigations have also been devoted to the study of the relationship between the peak intensities of SEP events and the parameters of the associated solar flares and CMEs (e.g. Dierckxsens et al. 2015, Grechnev et al., 2015, Trottet et al. 2015). However, longitudinal dependence of peak intensities of SEP events on associated flares have not been investigated in the papers (Dierckxsens et al., 2015, Grechnev et al., 2015, Trottet et al. 2015). The longitudinal dependence of peak intensities of SPEs on SXR peak flux has been investigated by Park et al. (2010). However, the longitudinal area were divided into E90-E30, E30-W30 and W30-W90 and only the CCs between peak intensities of SPEs and flare intensities in these three longitudinal areas have been calculated. It is evident that Park et al. (2010) have not calculated the CC between SXR peak flux and peak intensities of SPEs in the well connected region, and the relationship between SXR fluence and peak intensities of SPEs has not been investigated in their paper.

It has been accepted that SEPs accelerated by CME-driven shock can be observed in a very large longitudinal area, while flare-accelerated particles can only be observed in a small longitudinal area, especially in the longitudinal area well connected with the source location of associated SEP event. When a solar flare is an eruptive flare, the accompanied CME will open the magnetic field over the associated active region (AR), leading to the flare-accelerated particles can escape from the AR and then enter the interplanetary space. Because the magnetic field lines over an AR are very complicated and SEPs not only can propagate along the magnetic field lines, but also can propagate along the direction perpendicular to the magnetic field lines (Bieber et al., 2004, Qin, 2007, Qin et al. 2013, 2014, 2015), leading to flare-accelerated particles not only can be observed in the longitudinal area well connected with the SEP source region, but also can be observed in the longitudinal area outside the well connected region. However, the largest flux of flare-accelerated particles can only be observed in the longitudinal area well connected with SEP source location. When a large gradual SEP event happens, if a lot of satellites can be used to observe the SEP flux at every magnetic field line, then it is easy to check whether the SEP flux is longitudinal dependent and reaches its largest flux in the longitudinal area well connected with the SEP source location, which can be used to judge whether associated flares contribute to the production of SEPs in a large gradual SEP event. However, there has been no this kind of SEP data. Statistical correlation analysis can also be used to judge whether flares contribute to the production of SEPs. If flares really contribute to the production of SEPs in large gradual SEP events, then flares should have good correlation with the peak intensities of SEP events in the well connected region, while flares should have poor correlation with the peak intensities of SEP events in the longitudinal area outside the well connected region. The classical and partial correlation analyses for the relationship between the peak intensities of E≥100 MeV protons and the parameters of associated flares and CMEs in the well connected region and in the longitudinal area outside the well connected region have been investigated.

The results suggest that for SEP events with source location in the well connected region, E≥100 MeV protons may be mainly accelerated by the concurrent flares (Le et al., 2017).

In this paper, the relationship between the parameters of flares and CMEs and the peak intensities of protons with different energies lower than 100 MeV in the well connected region and in the longitudinal area outside the well connected region will be investigated. This is the motivation of the paper. Data sources and definitions are presented in Section 2. The classical correlation analysis is presented in section 3. Section 4 is the partial correlation analysis. Section 5 is the summary and discussion and conclusion is presented in final section.

2 DATA SOURCES AND DEFINITIONS

A large gradual SEP event, or a solar protons event (SPE), is defined as the proton peak flux is 10 pfu (particle flux unit, particle cm^{-2} sr^{-1} s^{-1}) in the E>10 MeV channel measured by GOES spacecraft during a solar energetic particle (SEP) event accompanied by both a fast coronal mass ejection and a long duration SXR flare. When a large gradual SEP event happens, the flux of protons with different energy, such as E>10 MeV, E>30 MeV and E>50 MeV protons, may increase at almost the same time, however, the peak fluxes of protons with different energies are different.

The time integral of SXR flux for a flare, fluence (Φ_x), is defined as

$$\Phi_x = \int_{t_s}^{t_e} [f(t) - f(t_s)]dt, \tag{1}$$

where f(t) is the SXR flux, t_s and t_e are the start and end time of the SXR flare, respectively. Equation (1) indicates that SXR flux, from which the background has been subtracted, is integrated over the flare start to end times. The flare start, peak and end time has been defined by SEC/NOAA. The flare end time was defined as the time when SXR flux decayed to a middle point between SXR peak flux and background SXR flux (Kubo and Akioka 2004). Φ_x is related to the total energy released by the associated flare (Kubo and Akioka 2004, Chen et al. 2016), indicating that Φ_x is a better parameter describing the properties a SXR emission than SXR peak flux, and SXR fluence has better correlation with peak flux of 15-40 MeV protons than SXR peak flux (Trottet et al., 2015).

The SXR flare start, peak and end time, and the SXR fluence are obtained from (ftp://ftp.ngdc.noaa.gov/STP/space-weather/solar-data/). The peak intensity of E>10 MeV, E>30 and E>50 MeV protons observed by the Geostationary Operational Environmental Satellites (GOES) during solar cycle 23 were ever obtained from the website: (http://spidr.ngdc.noaa.gov/spidr/). To be noticed that the proton data observed by GOESs has been removed from the website site (http://spidr.ngdc.noaa.gov/spidr/). For the SPEs that occurred during solar cycle 23, the source location, the CME speed and flare intensity for each SPEs can be directed copied from the paper Cane (2010). The CME speed associated with SPE that occurred on 2005 January 20 used in the paper is 3242 km/s (Gopalswamy et al. 2005). The SPEs that occurred during solar cycle 24 are available from (http://umbra.nascom.nasa.gov/sdb/goes/particle/). The linear speed of a CME, V_{CME}, can be obtained from the CME catalogue (Yashiro, et al. 2004, http://cdaw.gsfc.nasa.gov/CME_list/) of Solar and Heliospheric Observatory/Large Angle Spectroscopic Coronagraph (SOHO/LASCO; Brueckneret al., 1995).

The source location that well magnetically connected with the Earth should be located in the west hemisphere of the Sun. 79 SPEs with source location in the west hemisphere that occurred during 1997-2014 were selected and listed in Table 1. In the Table, SPEs are numbered in column (1), the year and date of the events in column (2) and (3) respectively, the time when SXR flux reached its peak value in column (4), the location of the flare site in column (5), SXR peak flux, I_{SXR} , in column (6), SXR fluence in column (7), the linear speed of the CME in column (8), the peak intensity of E>10 MeV protons, I_{10}, in column (9), the peak intensity of E>30 MeV protons, I_{30}, in column (10), the peak intensity of E>50 MeV protons, I_{50}, in column (11). The CME speed associated with the SPE that occurred on 2005 January 20 estimated by Gopalswamy et al. (2005) is 3242 km/s, which will be used in the paper.

Table 1 The parameters of flares and CMEs associated large gradual SEP events during 1997-2014

No.	Year yyyy	Date mm/dd	Time hh:mm	Location	I_{SXR} (SXR peak flux)	$\Phi_{SXR}/10^3$ (ergs/cm^2)	V_{cme} (km/s)	I_{10} (pfu)	I_{30} pfu	I_{50} pfu
1	1997	11/04	05:55	S14W33	X2.1	5.60E-02	785	72	20.3	9.98
2	1997	11/06	11:50	S18W63	X9.4	3.60E-01	1556	490	189	115
3	1998	04/20	10:00	S43W90	M1.4	6.10E-02	1863	1700	384	103
4	1998	05/02	13:35	S15W15	X1.1	6.70E-02	938	150	48	24.3
5	1998	05/06	08:00	S11W65	X2.7	2.10E-01	1099	210	47.5	19.3
6	1998	11/05	19:00	N26W18	M8.4	1.10E-01	1118	11	0.94	0.328
7	1999	06/04	07:03	N17W69	M3.9	2.40E-02	2230	64	3.7	0.93
8	2000	04/04	15:41	N16W66	C9.7	2.30E-02	1188	55	0.99	0.321
9	2000	06/10	17:02	N22W38	M5.2	7.30E-02	1230	46	4.22	1.57
10	2000	07/14	10:24	N22W07	X5.7	7.50E-01	1674	24000	5680	1670
11	2000	07/22	11:34	N34W56	M3.7	7.00E-02	1230	17	4.22	1.57
12	2000	09/12	12:17	S17W09	M1.0	4.50E-02	1550	320	9.91	1.95
13	2000	11/08	23:28	N10W75	M7.4	2.10E-01	1738	14800	4440	1880
14	2000	11/24	14:55	N22W07	X2.3	1.60E-01	1245	100	14.7	4.98
15	2001	01/28	16:00	S04W59	M1.5	3.00E-02	916	49	6.03	1.89
16	2001	03/29	10:15	N14W12	X1.7	2.20E-01	942	35	3.93	1.15
17	2001	04/02	21:51	N18W82	X20	1.50E+00	2505	110	217	53.5
18	2001	04/10	05:26	S23W09	X2.3	3.00E-01	2411	355	14.4	3.69
19	2001	04/12	10:28	S19W42	X2.0	3.00E-01	1184	50	13.9	5.75
20	2001	04/15	13:50	S20W85	14.4	6.10E-01	1199	951	357	275
21	2001	04/26	13:12	N17W31	M7.8	9.20E-02	1006	57	0.5	0.298
22	2001	09/15	11:28	S21W49	M1.5	3.70E-02	478	11	1.26	0.45
23	2001	10/19	16:30	N15W29	X1.6	1.6E-01	901	11	2.59	1.03
24	2001	11/04	16:20	N06W18	X1.0	2.20E-01	1810	31700	1070	266
25	2001	11/22	22:30	S15W34	M9.9	3.10E-01	1437	18900	857	162
26	2001	12/26	05:40	N08W54	M7.1	3.40E-01	1446	779	331	180
27	2002	01/14	06:27	S28W83	M4.4	3.40E-01	1492	15	1.69	0.53
28	2002	02/20	06:12	N12W72	M5.1	2.20E-02	952	13	1.51	0.5
29	2002	03/15	23:10	S08W03	M2.2	1.30E-01	957	13	0.61	0.215
30	2002	03/18	02:31	S09W46	M1.0	4.50E-02	989	53	2.48	0.579
31	2002	03/22	11:14	S09W90	M1.6	4.90E-02	1750	16	0.45	0.162
32	2002	04/17	8:24	S14W34	M2.6	1.50E-01	1240	24	1.51	0.367
33	2002	04/21	01:51	S14W84	X1.5	6.00E-01	2393	2520	649	208
34	2002	05/22	03:54	S19W56	C5.0	2.50E-02	1557	820	10.2	1.15
35	2002	07/15	20:08	N19W01	M1.8	4.30E-02	1300	234	4.27	0.92
36	2002	08/14	02:12	N09W54	M2.3	6.00E-02	1309	26	0.77	0.36
37	2002	08/22	01:57	S07W62	M5.4	3.30E-02	998	36	12.6	5.98
38	2002	08/24	01:12	S08W81	X3.1	4.60E-01	1913	317	123	76.2
39	2002	11/9	13:23	S12W29	M4.6	4.80E-02	1838	404	12	1.46
40	2003	05/28	00:27	S07W17	X3.6	2.80E-01	1366	121	4.84	3.72
41	2003	05/31	02:24	S07W65	M9.3	8.50E-02	1835	27	6.79	2.92
42	2003	10/26	18:19	N02W38	X1.2	5.10E-01	1537	466	42.6	10.4
43	2003	10/29	20:49	S15W02	X10	8.70E-01	2029	3300	869	360
44	2003	11/02	17:15	S20W56	X8.3	9.10E-01	2598	1570	476	155
45	2003	11/04	19:29	S19W83	X28.0	2.30E+00	2657	353	59.3	15.3
46	2003	11/20	07:47	N01W08	M9.6	6.00E-02	669	13	0.82	0.26
47	2003	12/2	09:48	S13W65	C7.2	5.10E-03	1393	86	2.28	0.39
48	2004	04/11	04:19	S14W47	C9.6	1.30E-02	1645	35	1.04	0.4
49	2004	07/25	15:14	N08W33	M1.1	6.50E-02	1333	2086	29.1	1.86
50	2004	11/07	16:06	N09W17	X2.0	2.00E-01	1759	495	33.2	4.93
51	2004	11/10	02:13	N09W49	X2.5	1.60E-01	2000	300	49.5	13.2
52	2005	01/15	23:02	N15W05	X2.6	6.30E-01	2861	300	1.93	0.83
53	2005	01/17	09:52	N15W25	X3.8	8.40E-01	2547	400	1330	387
54	2005	01/20	07:01	N14W61	X7.1	1.30E+00	3242	1680	1550	1150
55	2005	07/13	14:49	N10W80	M5.0	2.00E-01	1423	10	1.16	0.32
56	2005	07/14	10:55	N10W89	X1.2	3.90E-01	2115	110	14.2	2.63
57	2005	08/22	17:27	S12W60	M5.6	1.70E-01	2378	330	27.2	4.8

3 CLASSICAL CORRELATION ANALYSIS AND RESULTS

Because our sample only comprises 79 SPEs, so we also use bootstrap method (Wall and Jenkins, 2012) to estimate the statistical uncertainty of the correlation coefficients, which was ever used by Trottet et

Table 2 is the continue of Table 1

No.	Year yyyy	Date mm/dd	Time hh:mm	Location	I_{SXR} (SXR peak flux)	$\Phi_{SXR}/10^3$ (ergs/cm^2)	V_{cme} (km/s)	I_{10} (pfu)	I_{30} pfu	I_{50} pfu
58	2006	12/13	02:40	S06W24	X3.4	5.10E-01	1774	698	372	239
59	2006	12/14	22:15	S05W31	X1.5	1.20E-01	1042	215	42.3	13.5
60	2010	08/14	10:05	N17W52	C4.4	9.90E-03	1205	14	1.69	0.63
61	2011	03/07	20:12	N24W59	M3.7	1.20E-01	2125	50	4.66	0.82
62	2011	06/07	06:41	S21W64	M2.5	4.40E-02	1255	72	24.5	12.8
63	2011	08/04	03:57	N15W49	M9.3	5.40E-02	1315	96	20.2	7.79
64	2011	08/09	08:05	N17W83	X6.9	1.90E-01	1610	26	15.4	8.65
65	2011	11/26	07:10	N08W49	C1.2	5.30E-03	933	80	2.91	0.56
66	2012	01/23	03:59	N28W36	M8.7	2.00E-01	2175	6310	422	73
67	2012	01/27	18:37	N27W71	X1.7	3.20E-01	2508	796	136	43.5
68	2012	03/13	17:41	N18W62	M7.9	2.40E-01	1884	469	71.8	21.2
69	2012	05/17	01:47	N12W89	M5.1	9.90E-02	1582	255	124	78.3
70	2012	07/06	23:08	S18W50	X1.1	4.30E-02	1828	25	5.11	2.06
71	2012	07/12	16:49	S16W09	X1.4	4.60E-01	885	96	3.49	0.96
72	2012	07/17	17:15	S17W75	C9.9	2.10E-01	958	136	14.6	4.67
73	2012	09/27	23:57	N08W41	C3.7	9.40E-03	1035	28	3.24	0.6
74	2013	05/22	13:32	N15W70	M5.0	1.40E-01	1466	1660	125	22.9
75	2013	09/29	23:37	N15W40	C1.3	1.10E-02	1179	182	8.81	1.54
76	2014	01/07	18:32	S15W11	X1.2	2.50E+00	1830	1033	185	42.6
77	2014	02/20	07:55	S15W67	M3.0	6.30E-02	948	22	6.67	3.59
78	2014	04/18	13:03	S16W41	M7.3	1.10E-01	1208	58	5.77	2.44
79	2014	09/10	17:45	N16W06	X1.6	3.80E-01	1425	126	7.89	3.19

al.(2015). The correlation coefficient was calculated for N pairs of values chosen at random within the set of N observations. This procedure was repeated 5000 times.

3.1 Correlation between SEPs and SXR peak flux

The source location of flare-accelerated particles are mainly distributed in the longitudinal area ranged from W40 to W70, which can be seen from Figure 2.3 in the paper of Reames (1999). The CCs between peak intensities of SEP events and SXR peak flux in three longitudinal areas: W0-W39, W40-W70 and W71-W90 have been derived and shown in Figure 1 for E>10 MeV protons, Figure 2 for E>30 MeV and Figure 3 for E>50 MeV protons respectively.

We can see from Figure 1 that the CCs between I_{10} and I_{SXR} in the three longitudinal areas W0-W39, W40-W70 and W71-W90 are 0.24±0.17, 0.43±0.15 and 0.26±0.24 respectively. It is obvious that the CC between I_{10} and SXR peak flux is longitudinal dependent. The largest CC is only 0.43±0.15 in the well connected region, suggesting that I_{10} has only a weak correlation with I_{SXR} in the well connected region.

We can see from Figure 2 that the CCs between I_{30} and SXR peak flux in the three longitudinal areas W0-W39, W40-W70 and W71-W90 are 0.43±0.15, 0.71±0.09 and 0.35±0.22 respectively. It is evident that the CC between I_{30} and SXR peak flux is highly longitudinal dependent, and the CC between I_{30} and I_{SXR} reaches its largest value in the well connected region and then declines dramatically in the longitudinal area outside the well connected region.

Figure 3 shows that the CCs between I_{50} and I_{SXR} in the three longitudinal areas W0-W39, W40-W70 and W71-W90 are 0.54±0.13, 0.77±0.07 and 0.36±0.22 respectively. The correlation coefficient between I_{50} and I_{SXR} is highly longitudinal dependent, and the CC between I_{50} and I_{SXR} reaches its largest value in the well connected region and then declines dramatically in the longitudinal area outside the well connected region.

3.2 Correlation between SEPs and SXR fluence

To check whether the CCs between SXR fluence and the peak flux of SEP events are longitudinal dependent, and compare the CC between SXR fluence and peak intensities of SEP events with the one

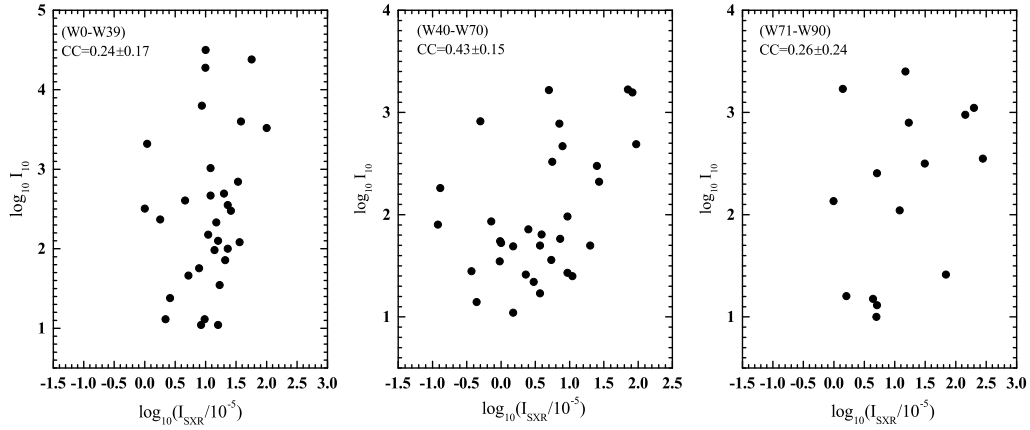

Fig. 1 Scatter (log-log) plots of I_{10} versus I_{SXR} in the three longitudinal areas respectively.

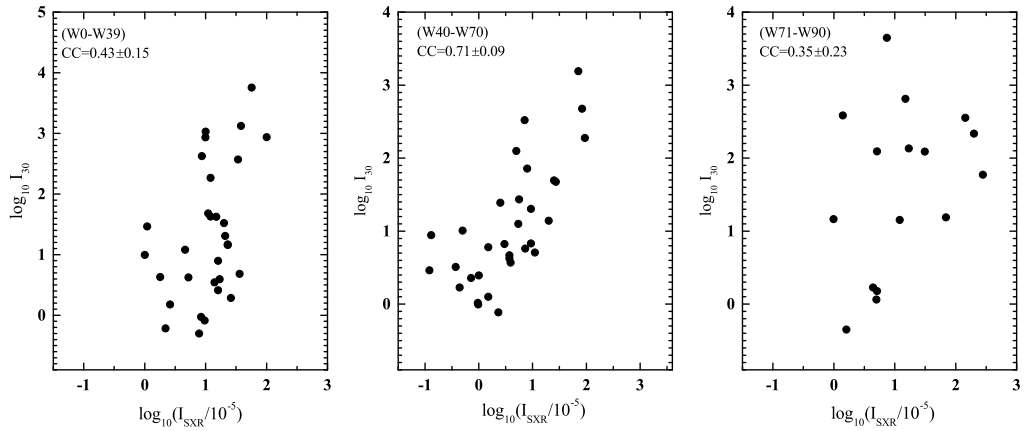

Fig. 2 Scatter (log-log) plots of I_{30} versus I_{SXR} in the three longitudinal areas respectively.

between SXR peak flux and the peak intensities of SEP events, the CCs between SXR fluence and peak intensities of SEP events have been derived and shown in Figure 4 for E>10 MeV, Figure 5 for E>30 MeV and Figure 6 for E>50 MeV protons respectively.

We can see from Figure 4 that the CCs between I_{10} and Φ_x in the three longitudinal areas W0-W39, W40-W70 and W71-W90 are 0.43±0.15, 0.58±0.12 and 0.39±0.22 respectively. Although the correlation between Φ_x and I_{10} is moderate in the well connected region, the CC between Φ_x and I_{10} is still highly longitudinal dependent. It evident that Φ_x has closer association with I_{10} than I_{SXR}.

We can see from Figure 5 that the CCs between I_{30} and Φ_x in three longitudinal areas W0-W39, W40-W70 and W71-W90 are 0.50±0.14, 0.80±0.06 and 0.37±0.22 respectively. It is evident that the CC between I_{30} and Φ_x is highly longitudinal dependent, and I_{30} has a good correlation with Φ_x in the

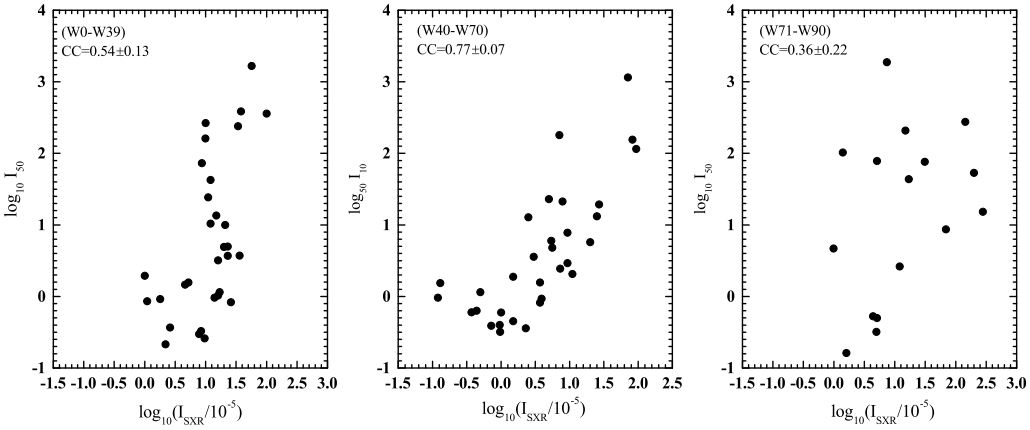

Fig. 3 Scatter (log-log) plots of I_{50} versus I_{SXR} in the three longitudinal areas respectively.

well connected region. The CC between Φ_x and I_{30} is larger than that between I_{SXR} and I_{30} in the well connected region, suggesting that Φ_x has closer association with I_{30} than I_{SXR}. The CC between I_{30} and Φ_x is larger than the one between I_{10} and Φ_x in the well connected region, suggesting that I_{30} has closer association with Φ_x than I_{10}.

Figure 6 shows that the CCs between I_{50} and Φ_x in the three longitudinal areas W0-W39, W40-W70 and W71-W90 are 0.54±0.13, 0.83±0.06 and 0.13±0.28 respectively. It is evident that the CC between I_{50} and Φ_x is highly longitudinal dependent. The CC between I_{50} and Φ_x is larger than the one between I_{50} and I_{SXR} in the well connected region, suggesting that I_{50} has closer association with Φ_x than I_{SXR}. The CC between I_{50} and Φ_x is larger than the one between I_{30} and Φ_x in the well connected region, suggesting that I_{50} has closer association with Φ_x than I_{30}.

3.3 Correlation between peak intensities of SEP events and CME speeds

The CCs between the speeds of CMEs and the peak intensities of SEP events with different energies in three longitudinal areas W0-W39, W40-W70 and W71-W90 have been derived and shown in Figures 7 for E>10 MeV protons, Figure 8 for E>30 MeV protons and Figure 9 for E>50 MeV protons respectively.

We can see from Figure 7 that CCs between I_{10} and V_{CME} in the three longitudinal areas W0-W39, W40-W70 and W71-W90 are 0.67±0.10, 0.56±0.12 and 0.45±0.21 respectively. The CC between V_{CME} and I_{10} is slightly longitudinal dependent and the CC reaches its largest value in the longitudinal W0-W39.

We can see from Figure 8 that CC between I_{30} and V_{CME} in the three longitudinal areas W0-W39, W40-W70 and W71-W90 are 0.54±0.10, 0.53±0.13 and 0.40±0.21 respectively. The CC in the longitudinal area W0-W39 is almost the same as the CC in the longitudinal area W40-W70.

Figure 9 shows that CCs between I_{50} and V_{CME} in the three longitudinal areas W0-W39, W40-W70 and W71-W90 are 0.50±0.14, 0.48±0.14 and 0.34±0.23 respectively. The difference between the CC in the longitudinal area W0-W39 and the CC in the longitudinal area W40-W70 is only 0.02, which can be ignored.

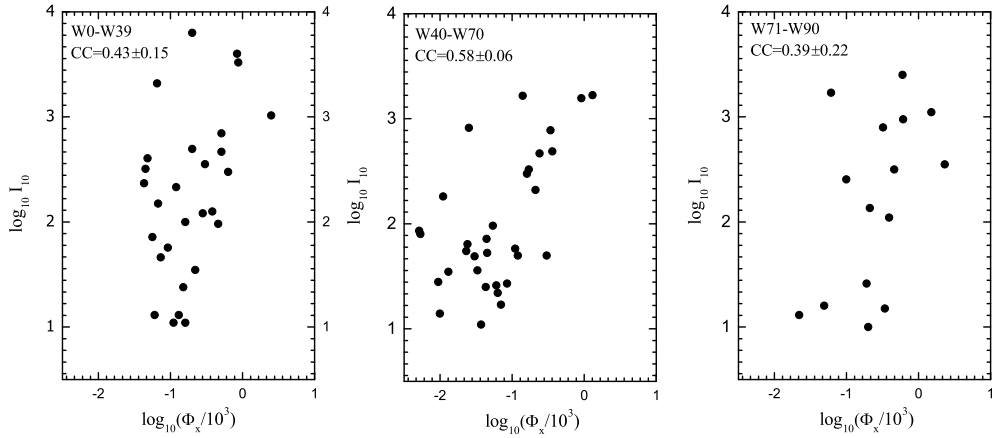

Fig. 4 Scatter (log-log) plots of I_{10} versus Φ_x in the three longitudinal areas respectively.

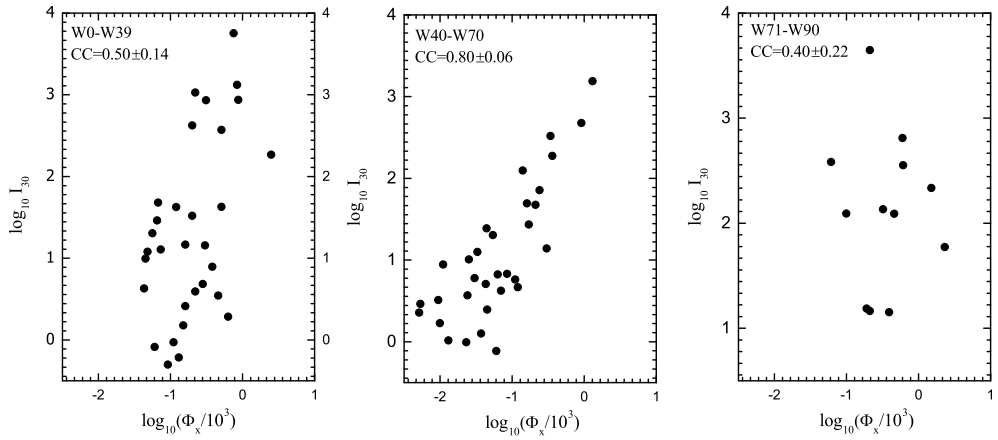

Fig. 5 Scatter (log-log) plots of I_{30} versus Φ_x in the three longitudinal areas respectively.

4 PARTIAL CORRELATION ANALYSIS

Partial correlation between two variables is considered by nullifying the effects of the third (or fourth, or more) variable upon the variables being considered, which has been used by Trottet et al. (2015) to analyze the correlation between peak intensities of 15-40 MeV protons and the parameters of the associated solar activities. To investigate CME speed, SXR peak flux and SXR fluence independently affect the peak intensities of E>10 MeV, E>30 MeV and E>50 MeV protons in the well connected region, the partial correlation coefficients between the peak intensities of E>10 MeV, E>30 MeV and E>50 MeV protons and the parameters of associated solar activities, together with the statistical uncertainties from

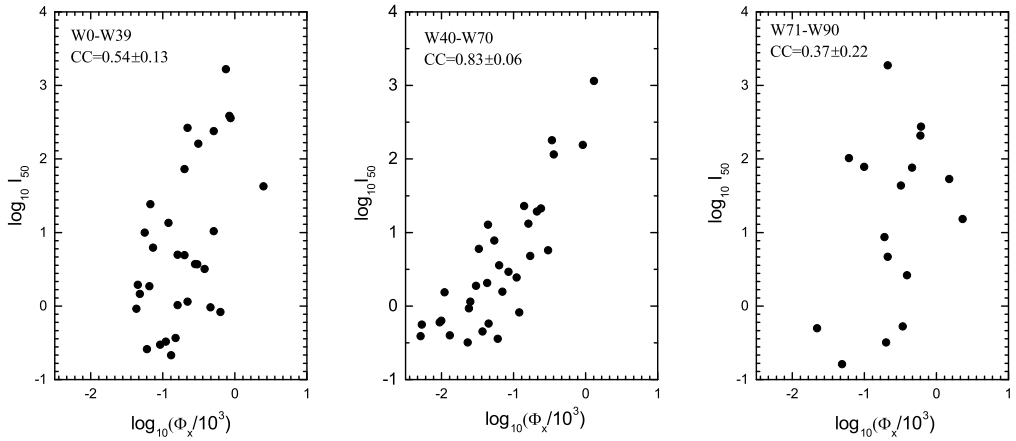

Fig. 6 Scatter (log-log) plots of I_{50} versus Φ_x in the three longitudinal areas respectively.

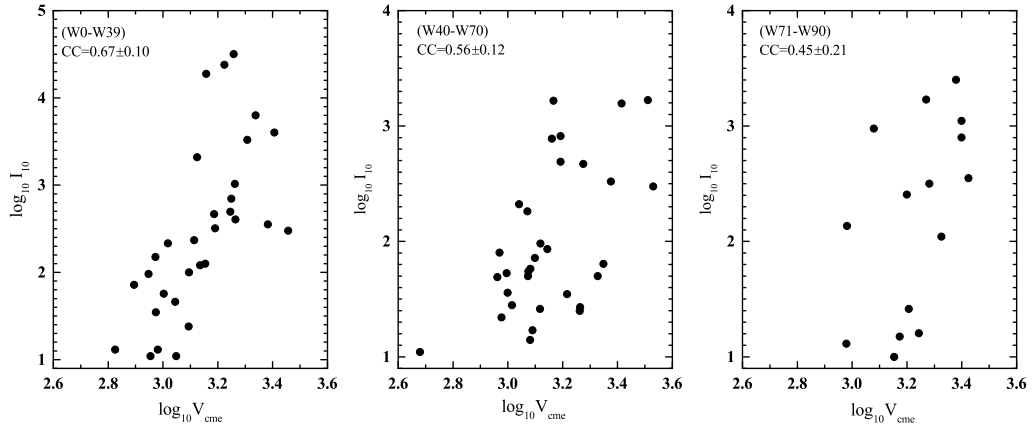

Fig. 7 Scatter (log-log) plots of I_{10} versus V_{CME} in the three longitudinal areas respectively.

the bootstrap method will be calculated. We use CC_p (X, Y) to indicate the partial correlation coefficient between parameters X and Y.

4.1 Partial correlation analysis for E>10 MeV protons

For SEP events with source location in the well connected region, $CC_p(\log_{10}I_{10}, \log_{10}V_{cme})$, $CC_p(\log_{10}I_{10}, \log_{10}I_{SXR})$ and $CC_p(\log_{10}I_{10}, \log_{10}\Phi_x)$ are 0.46±0.15, -0.36±0.16 and 0.51±0.14 respectively, suggesting that for the SEP events with source location in the well connected region, both CME speed and SXR fluence can significantly affect the peak intensities of E>10 MeV protons, while SXR peak flux makes no additional contribution.

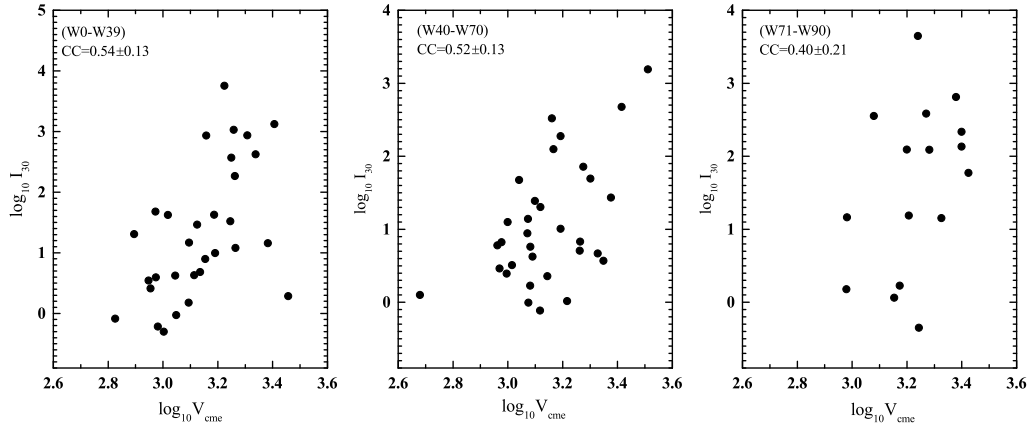

Fig. 8 Scatter (log-log) plots of I_{30} versus V_{CME} in the three longitudinal areas respectively.

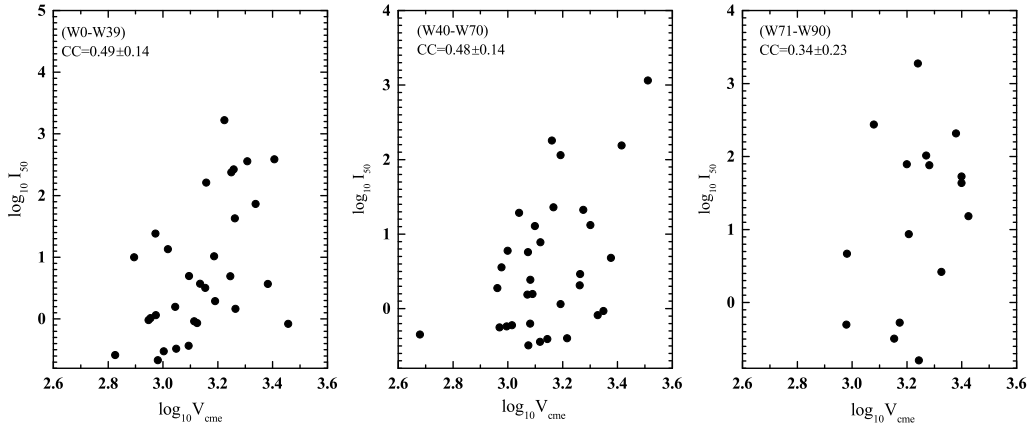

Fig. 9 Scatter (log-log) plots of I_{50} versus V_{CME} in the three longitudinal areas respectively.

4.2 Partial correlation analysis for E>30 MeV protons

For SEP events with source location in the well connected region, $CC_p(\log_{10}I_{30}, \log_{10}V_{cme})$, $CC_p(\log_{10}I_{30}, \log_{10}I_{SXR})$ and $CC_p(\log_{10}I_{30}, \log_{10}\Phi_x)$ are 0.26±0.18, -0.06±0.19 and 0.52±0.14 respectively. It is evident that Φ_x has much better correlation with peak intensity of E>30 MeV protons than V_{CME}, suggesting that for the SEP events with source location in the well connected region, only Φ_x can significantly affect the peak intensities of E>30 MeV protons, while CME shock just make small contribution to the peak intensities of E>30 MeV protons, and I_{SXR} makes no additional contribution the peak intensities of E>30 MeV protons.

4.3 Partial correlation analysis for E>50 MeV protons

For SEP events with source location in the well connected region, $CC_p(\log_{10}I_{50}, \log_{10}V_{cme})$, $CC_p(\log_{10}I_{50}, \log_{10}I_{SXR})$ and $CC_p(\log_{10}I_{50}, \log_{10}\Phi_x)$ are 0.11±0.19, 0.11±0.19 and 0.49±0.14 respectively, suggesting that for the SEP events with source location in the well connected region, only SXR fluence can significantly affect the peak intensities of E>50 MeV protons, while both SXR peak flux and CME speed make no additional contribution to the peak intensities of E>50 MeV protons.

5 SUMMARY AND DISCUSSION

5.1 If the source locations of SEP events are not well connected with the Earth, GOES spacecraft is located in a poor position to observe the particles accelerated by concurrent flares. However, if the source locations of SEP events are well connected with the Earth, GOES spacecraft is located in a good position to observe flare-accelerated particles. This suggests that if flares really contribute to the production of SEPs in the large gradual SEP events, then the correlation coefficient between flares and the peak intensities of SEP events should be longitudinal dependent, and the CC between flares and SEPs should reach its largest value in the well connected region and decline dramatically in the longitudinal area outside the well connected region. The results of the paper suggest that flares really contribute to production of E>10 MeV, E>30 MeV, E>50 MeV protons.

5.2 By comparing Figure 1 with Figure 7, we can find that the CC between speeds of CMEs and I_{10} is always larger than the CC between SXR peak flux and I_{10} in the same longitudinal area, suggesting that for E>10 MeV protons, CME speed is more important than flare intensity, which is consistent with the result obtained in the paper of Park et al. (2012).

5.3 For E>10 MeV, E>30 MeV and E>50 MeV protons with source location in the well connected region, the classical correlation analyses show that the CC between SXR fluence and peak intensities of SEPs is always larger than that between SXR peak flux and peak intensities of SEPs, suggesting that SXR fluence always has closer association with the peak intensities of SEP events than SXR peak flux, namly that SXR fluence is an more important parameter describing the relationship between SXR emission and SEP events than SXR peak flux.

5.4 For E>10 MeV protons, the combination of classical correlation and partial correlation analyses shows that in the well connected region, both flare and CME shock are effective accelerator for E>10 MeV protons. For E>30 MeV protons, the combination of classical correlation and partial correlation analyses shows that in the well connected region, E>30 MeV protons can be accelerated by both concurrent flares and CME shocks, however, E>30 MeV protons may be mainly accelerated by the concurrent flares. For E>50 MeV protons, the combination of classical correlation and partial correlation analyses shows that in the well connected region, E>50 MeV protons may be only accelerated by the concurrent flares.

5.5 The outstanding property of flare-accelerated particles is that the flux of the particles accelerated by flares is highly longitudinal or the correlation coefficient between flares and the peak intensities of SEP events are highly dependent on heliolongitude. If we do not divide the SEP events into three longitudinal region shown in the paper, the longitudinal dependence of SEP events on the associated flares can not be found, which has been proved by Le et al. (2017). To be noticed that the well connected region may not be exactly in the longitudinal area ranged from W40 to W70. The CCs between flares and the peak intensities of SEP should be calculated in much more longitudinal areas to precisely look for the well connected region if the sample number of large SEP events is large enough.

5.6 To be noticed that the flares, in some cases, not accompanied by SEP events if the flares are not accompanied by CMEs. Klein et al. (2010) suggested that the flare-accelerated particles might be trapped in the flare site if the radio emission at decimeter and longer wavelength are absent. In other words, the flare is confined. If the solar flare is eruptive, the CMEs can open quite amount of magnetic configuration above the solar active region and make it easier for the escape of flare-accelerated particles.

6 CONCLUSION

6.1 The classical correlation analysis shows that in the well connected region, higher protons have closer association with concurrent flares, while lower energy protons have better correlation with the speeds of associated CMEs, suggesting that flares are effective accelerator for higher energy protons, while CME shocks are effective accelerator for lower protons.

6.2 The combination of classical correlation analysis and partial correlation analysis suggests that for SEP events with source location in the well connected region, CME shock is only an effective accelerator for E<30 MeV protons, while flares are not only effective accelerators for E<30 MeV protons, but also for E>30 MeV protons, and E>30 MeV protons may be mainly accelerated by concurrent flares.

Statistical results are usually given for the majority of the cases. The results of the paper do not rule out the possibility that for SEP events with source locations in the well connected region, shock driven by associated CME may paly key role in the production of E>30 MeV protons and even for higher energy protons. The discussion of shock geometry and intensity, and whether this kind of shock is well connected with the Earth is beyond the scope of the paper.

Acknowledgements We are very grateful to the anonymous referee for her/his reviewing of the paper and for helpful suggestions. We thank Dr Jingtian Lv for helping us to provide Figure 10. This work was jointly funded by the National Basic Research Program of China (973 Program, Grants 2012CB957801 and 2014CB744203), the National Natural Science Foundation of China (grants 41074132, 41274193, 41474166, 41304144, 11303017, 11533005), the National Standard Research Program (Grant 200710123). The SXR data including the flare start, peak and end time, and the SXR fluence were obtained freely from NOAA (ftp://ftp.ngdc.noaa.gov/STP/space-weather/solar-data/solar-features/solar-flares/x-rays/goes). The data of SPEs that occurred during solar cycle 23 were ever obtained freely from NOAA (http://spidr.ngdc.noaa.gov/spidr), while the data of SPEs that occurred during solar cycle 24 were also obtained freely from NOAA (http://umbra.nascom.nasa.gov/sdb/goes/particle). The linear speed of each CME, which was funding for the early phase of the catalog was provided by AFOSR and NSF. Currently, the catalog resides at the CDAW Data Center at Goddard Space Flight Center and is supported by NASA's Living with a Star program and the SOHO project, were obtained freely from the CME catalogue (http://cdaw.gsfc.nasa.gov/CME_list)

References

Andriopoulou, M., Mavromichalaki, H., Plainaki, C., Belov, A., and Eroshenko, E. 2011, Sol. Phys., 269, 155

Aschwanden, M. J. 2012, Space Sci. Rev., 171, 3

Aurass H., Mann G., Rausche G., and Warmuth A. 2006, A&A,457, 681

Bazilevskaya, G. A. 2009, Adv. Space Res., 43, 530

Bieber J. W., Matthaeus W. H., Shalchi A. and Qin G. 2004, Geophys. Res. Lett., 31, L10805

Brueckner, G. E., Howard, R. A., Koomen, M. J., et al. 1995, Sol. Phys., 162, 357

Cane, H. V.; Richardson, I. G.; von Rosenvinge, T. T., 2007, SSR, 130, 301

Cane, H. V., I. G. Richardson, and T. T. von Rosenvinge 2010, J. Geophys. Res., 115, A08101

Chen, Yulin, Le, Guiming, Lu, Yangping, Chen, Minhao, Ding, Liuguan, Yin, Zhiqiang, 2016, Ap&SS, 361, 40.

Dierckxsens M., Tziotziou K., Dalla S., Patsou I., Marsh M.S., Crosby N.B., Malandraki O, Tsiropoula G. 2015, Sol. Phys., 290, 841

Firoz, K. A., Gan,W.-Q., Moon, Y. J., & Li, C., 2012, ApJ, 758, 119.

Gopalswamy,N., Xie, H.,Yashiro, S.,&Usoskin, I. 2005, Proc. 29th Int. Cosmic Ray Conf. (Pune), 1, 169

Grechnev, V. V., Kurt, V. G., Chertok, I. M., et al. 2008, Sol. Phys., 252, 149

Grechnev, V. V.; Kiselev, V. I.; Meshalkina, N. S.; Chertok, I. M. 2015, Sol. Phys., 290, 2827

Kallenrode M-B, J. Phys. G: Nucl. Part. Phys. 29, 965

Klein, K.-L., Trottet, G., Klassen, A. 2010, Sol. Phys., 263, 185.

Klein K.-L., Masson S., Bouratzis C., Grechnev V., Hillaris A. and P. Preka-Papadema, 2014, å, 572, A4

Kubo, Y., and M. Akioka 2004, Space Weather, 2, S01002

Kouloumvakos A., Nindos A., Valtonen E., Alissandrakis C.E., Malandraki O., Tsitsipis P., Kontogeorgos A., Moussas X., Hillaris A. 2015, A&A, 580, A80

Le, Gui-Ming,Yuhua Tang and Yanben Han, 2006, Chin. J. of Astron. Astrophys., 6, 751.

Le, Gui-Ming, Li Chuan, Yang Hui-Geng, Chen Yu-Lin, Yang Xing-Xing and Yin Zhi-Qiang, 2013, Research in Astron. Astrophys. (RAA), 13, 1219

Le, Gui-Ming, Li Chuan, Tang, Yu-Hua, Ding-Liuguan, Yin, Zhi-Qiang, Chen, Yu-Lin, Lu, Yang-Ping, Chen, Min-Hao, Li, Zhong-Yi, 2016, Research in Astron. and Astrophys. (RAA), 16, 14(12pp).

Le, Gui-Ming, Li, Chuan and Zhang, Xuefeng, 2017, *Research in Astron. and Astrophys. (RAA)*,7, 73

Li, C., Tang Y. H., Dai Y., Fang C. and Vial J.C. 2007a, A&A, 472, 283.

Li, C., Tang Y. H., Dai Y., Zong, W. G. and Fang C. 2007b, A&A, 461, 1115.

Li, C.; Dai, Y., Vial, J.-C., Owen, C. J.; Matthews, S. A., Tang, Y. H., Fang, C., Fazakerley, A. N. 2009, A&A, 503, 1013

Masson, S., Klein, K.-L., Bütikofer, R., Flückiger, E.; Kurt, V., Yushkov, B., Krucker, S. 2009, Sol. Phys., 257, 305

Miroshnichenko, L. I., Klein K.-L., Trottet G., Lantos P., Vashenyuk E. V., Balabin Y. V., and Gvozdevsky B. B. 2005, J. Geophys. Res., 110, A11S90

Park, J., Y.J. Moon, D. H. Lee, and S. Youn 2010, J. Geophys. Res., 115, A10105

Park, J., Y.J. Moon,and N. Gopalswamy 2012, J. Geophys. Res., 117, A08108

Perez-Peraza, J., Vashenyuk, E. V., Miroshnichenko, L. I., Balabin, Yu. V., and Gallegos-Cruz, A. 2009, Astrophys. J., 695, 865

Qin G. 2007, ApJ, 656, 217

Qin G., Wang Y, Zhang M. and Dalla S. 2013, ApJ, 766,74

Qin G, and Zhang L.-H. 2014, ApJ, 787, 12

Qin G. and Wang Y., 2015, ApJ, 809, 177

Reames, D. V. 1999, Space Sci. Rev., 90, 413

Simnett, G. M. 2006, A&A, 445, 715

Wall, J.V., Jenkins, C. R. 2012, Cambridge and New York, Chap. 6.6

Trottet, G., Samwel, S., Klein, K.-L., Dudok de Wit, T., Miteva R. 2015, Sol. Phys., 290(3), 819

Tylka, A. J., Cohen, C. M. S., Dierich, W. F., Lee, M. A., Maclennan C.G., Mewaldt, R. A, C. K. Ng, C. K. and D. V. Reames, D. V. 2005, ApJ, 625, L474.

Yashiro, S., Gopalswamy, N., Michalek, G., St. Cyr, O.C., Plunkett, S.P., Rich, N.B., Howard, R.A. 2004, J. Geophys. Res., 109, A07105

This paper was prepared with the RAA LaTeX macro v1.2.